THE JOURNAL OF PHYSICAL CHEMISTRY A

ARTICLE

pubs.acs.org/JPCA

Kinetics of Hydrogen Bonding between Anthracene Urea Derivatives and Anions in the Excited State

Satomi Ikedu, Yoshinobu Nishimura, and Tatsuo Arai*

Graduate School of Pure and Applied Sciences, University of Tsukuba, 1-1-1 Tennoudai, Tsukuba, Ibaraki 305-8571, Japan

Supporting Information

ABSTRACT: Urea compounds are useful anion sensors due to their hydrogen-bonding capabilities. We investigated the emissive properties of complexes consisting of urea−anthracene (*n*PUA, *n* = 1, 2) host compounds and acetate anions held as guests through intermolecular hydrogen bonding. The kinetics of a new emission band formed by conformational changes in the excited singlet state were revealed. The new band is thought to arise from a charge-transfer interaction between the anthracene and urea moieties after intermolecular hydrogen-bond reconfiguration in the excited state, with rate constants of 2.4×10^9 and 4.0×10^7 s^{-1} for 1PUA and 2PUA, respectively.

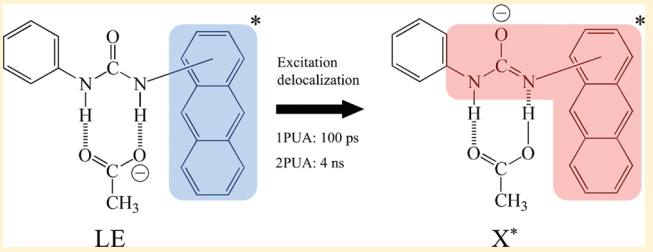

INTRODUCTION

Much effort has been devoted to the development of anion sensors in various fields.[1] Urea has been used as an anion receptor since the discovery of remarkable properties that contribute to its usefulness in this area.[2,3] The hydrogen-bonding capability of urea compounds containing chromophore groups allows for spectroscopic detection of anions including phosphate, acetate, and sulfate ions.[4−12] However, there have been few studies on the kinetics of chromophores interacting with anions in the excited singlet state, or on the origin of a new emission band additional to that observed in the absence of anions. The aim of this study was to elucidate the fluorescence behavior of urea compounds containing an anthracene moiety as a fluorophore by using time-resolved fluorescence spectroscopy, which enabled us to estimate the rate constants of elemental processes involved in hydrogen-bonding interactions in the excited singlet state.

Previous investigations have dealt with the photochemistry of urea derivatives containing an anthracene fluorophore and a urea moiety which acts as a probe for anions such as bromide or acetate.[13] In a previous paper, such a compound, 1-anthracen-9-yl-3-phenylurea (9PUA), was studied in the presence of a variety of anions in dimethyl sulfoxide (DMSO) solution. 9PUA was found to show dual fluorescence spectra, maximized at 450 and 580 nm, in the presence of acetate anions, while fluorescence enhancement was observed only in the presence of bromide anions. Thus, acetate anions were found to interact with 9PUA followed by the formation of a new emissive species with a large Stokes shift of 8300 cm^{-1}. Since the acetate anions appeared not to form a charge-transfer state with the urea moiety of 9PUA, the newly formed emissive state ($^1X^*$) was suggested to be intrinsically different from the locally excited (LE) state of 9PUA, because of the large Stokes shift. A plausible emissive structure, based on proton transfer from the urea moiety in the LE state to the acetate anion, was proposed.

Since the interaction of the urea moiety at the 1- or 2-position of anthracene was expected to be different from that at the 9-position, we synthesized the urea−anthracene compounds *n*PUA (*n* = 1, 2, where *n* is the substituted position of the parent anthracene; see Scheme 1) to investigate the emissive state. 1PUA and 2PUA exhibited absorption spectra similar to those of 1-aminoanthracene and 2-aminoanthracene, respectively.[14] *n*PUA also showed dual emission spectra in the presence of acetate anions in DMSO, indicating the formation of emissive species comparable to those of 9PUA. Interestingly, the rising component, which was attributed to a new emissive species in the presence of acetate anions, was observed at a longer wavelength, the time constant of which agreed well with the decay constant of the LE state. This is a specific phenomenon of 1PUA and 2PUA, since 9PUA has no rising component.

In this study, by taking advantage of spectroscopic techniques, we demonstrate that the interaction of *n*PUA with acetate anions and the formation of emissive species upon irradiation are dependent upon the substitution position. We also elucidate the rate constants in the excited singlet state on the basis of a two-state model and consistent with the steady-state emission spectra. It was found that the rate constant of $^1X^*$ formation was completely dependent on the substituted position of the anthracene moiety, with 1PUA forming $^1X^*$ 2 orders of magnitude faster than 2PUA.

EXPERIMENTAL METHODS

Methods. Absorption and fluorescence spectra were measured on Shimadzu UV-1600 and Hitachi F-4500 fluorescence spectrometers, respectively. Fluorescence decay measurements

Received: March 10, 2011
Revised: June 8, 2011
Published: June 20, 2011

Scheme 1. Structures of 1PUA and 2PUA

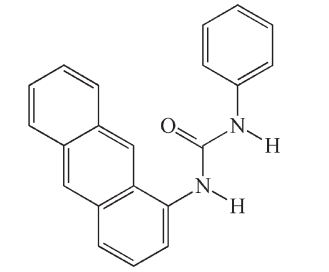

1PUA

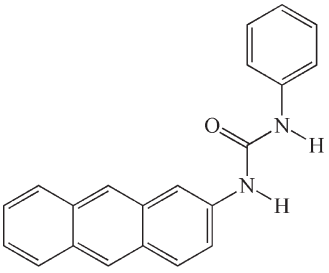

2PUA

were performed using a time-correlated single-photon counting method. Laser excitation at 375 nm was performed using a diode laser (PicoQuant, LDH-P-C-375) with a power control unit (PicoQuant, PDL 800-B), with a repetition rate of 2.5 MHz. The temporal profiles of the fluorescence decays were detected by a microchannel plate photomultiplier (Hamamatsu, R3809U) equipped with a TCSPC computer board module (Becker and Hickl, SPC630). The full width at half-maximum (fwhm) value of the instrument response function was 51 ps.[15] The values of χ^2 and the Durbin−Watson parameters were used to determine the quality of the fit obtained by nonlinear regression.[16] DMSO (spectroscopic grade, Wako Pure Chemical Industries, Japan) was used as a solvent without further purification. Acetate anions were in the form of tetrabutylammonium acetate (TBAAc), which contains a tetrabutylammonium cation (Sigma-Aldrich, Japan). All measurements were carried out at room temperature under an Ar atmosphere. The concentrations were adjusted so that the absorption maximum of the excitation wavelength was about 0.1 for each sample. Density functional theory (DFT) calculations were performed using the Spartan '04 program (Wavefunction, Inc., Irvine, CA, USA).

Synthesis. *1-Aminoanthracene*[17,18]. A mixture of 1-aminoanthraquinone (1.66 g, 7.44 mmol) and NaOH (106.4 mg, 2.66 mmol) in 2-propanol (60 mL) was bubbled with N_2 for 15 min before the addition of $NaBH_4$ (2.86 g, 75.6 mmol), and the mixture was refluxed for 100 h at 80−90 °C under N_2. The addition of another portion of $NaBH_4$ (0.56 g, 14.8 mmol) to the mixture followed by 15 h of stirring gave a precipitate, which was filtered off, washed with water, and dried in vacuo. The residue was dissolved in chloroform and dried over anhydrous Na_2SO_4 before being concentrated in a rotary evaporator under reduced pressure. This yielded 532 mg of 1-aminoanthracene as a pale yellow solid, which was used for the subsequent step without further purification due to difficulties with recrystallization. ^{1}H NMR ($CDCl_3$, 270 MHz): δ 8.39 (d, 2H, J = 3.5 Hz, anthryl), 7.99 (t, 2H, J = 8.5 Hz, anthryl), 7.52−7.47 (m, 3H, anthryl), 7.31 (d, 1H, J = 8.1 Hz, anthryl), 6.76 (d, 1H, J = 7.0 Hz, anthryl), 4.31 (s, 2H, $-NH_2$).

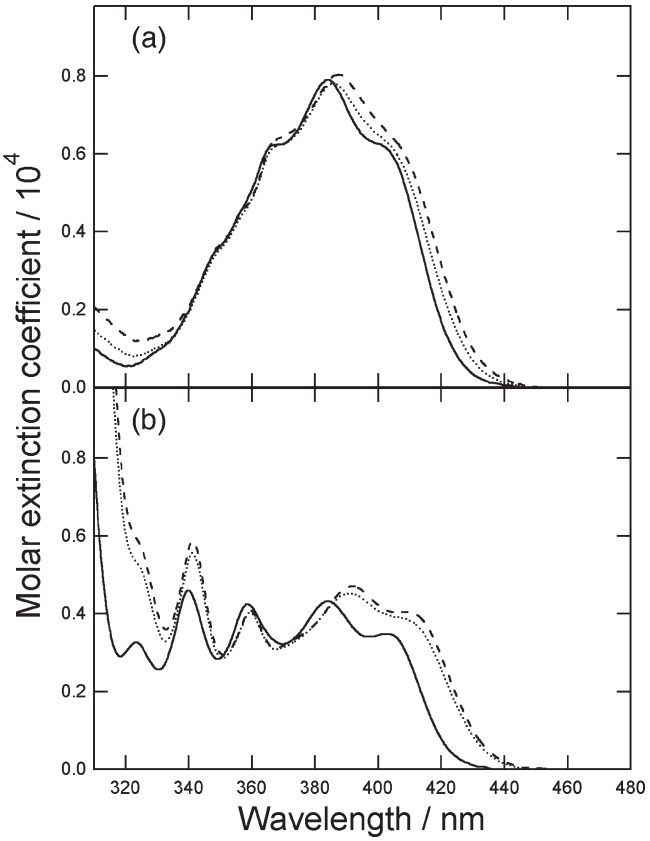

Figure 1. Changes in the absorption spectra of (a) 1PUA and (b) 2PUA in the presence of TBAAc. [TBAAc] = 0 (—), 1 (· · ·), and 10 mM (---).

1-Anthracen-1-yl-3-phenylurea (1PUA)[9]. 1-Aminoanthracene (161.6 mg) and phenylisocyanate (90 μL, 0.831 mmol) were stirred in dry tetrahydrofuran (THF; 8 mL) at room temperature under N_2 for 17 h. After the addition of another portion of phenylisocyanate (90 μL, 0.831 mmol) dissolved in dry THF (4 mL) to the mixture, and 17 h stirring, the solvent was evaporated under reduced pressure, and the residue was dried and purified by recrystallization in ethanol to yield 1PUA (45.2 mg, 0.145 mmol) as a yellow solid. ^{1}H NMR (DMSO-d_6, 270 MHz): δ 9.12 (s, 1H, −NH), 8.97 (s, 1H, −NH), 8.76 (s, 1H, anthryl), 8.60 (s, 1H, anthryl), 8.12−8.03 (m, 2H, anthryl), 8.02 (d, 1H, J = 9.1 Hz, anthryl), 7.81 (d, 1H, J = 8.4 Hz, anthryl), 7.57−7.46 (m, 5H, anthryl and phenyl), 7.33 (t, 2H, J = 6.9 Hz, phenyl), 7.00 (t, 1H, J = 7.3 Hz, phenyl); ^{13}C NMR (DMSO-d_6, 67.5 MHz): δ 152.8, 139.6, 133.9, 131.7, 130.9, 130.7, 128.8, 128.1, 127.7, 126.6, 125.8, 125.4, 125.1, 122.9, 121.8, 119.7, 118.0, 115.7; Anal. Calcd for $C_{16}H_{21}N_2O$: C, 80.75; H, 5.16; N, 8.97; found: C, 80.67; H, 5.40; N, 8.83.

2-Aminoanthracene[17,18]. A mixture of 2-aminoanthraquinone (2.99 g, 13.4 mmol) in 2-propanol (200 mL) was bubbled with N_2 for 15 min before addition of $NaBH_4$ (6.31 g, 168 mmol), and the mixture was refluxed for 66 h at 80 °C under N_2. The solution was then poured into water, and the resulting precipitate was filtered off, washed with water and 2-propanol, and dissolved in ethanol. The solution was then filtered again to exclude impurities and concentrated in a rotary evaporator under reduced pressure. The residue was recrystallized from ethanol

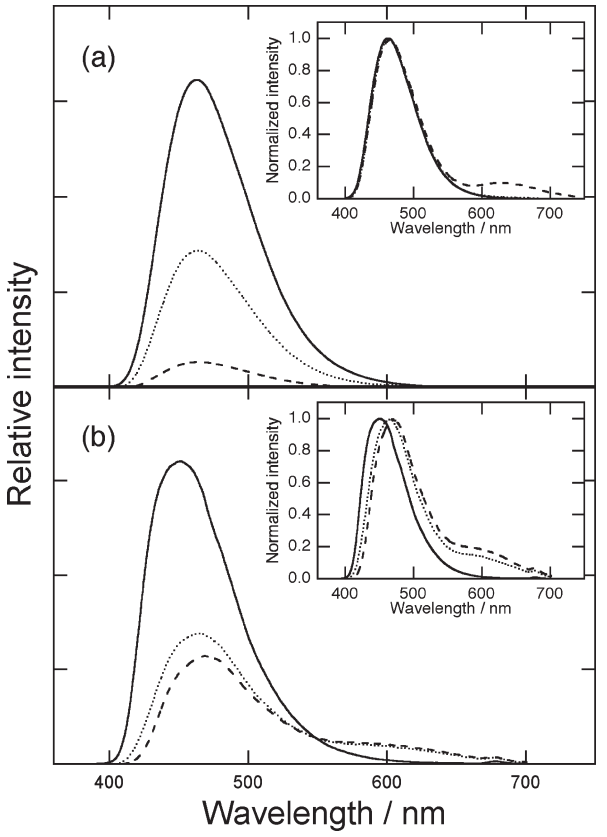

Figure 2. Changes in the fluorescence spectra of (a) 1PUA and (b) 2PUA in the presence of TBAAc. [TBAAc] = 0 (—), 1 (···), and 10 mM (---). The insets show normalized spectra at maximum intensity.

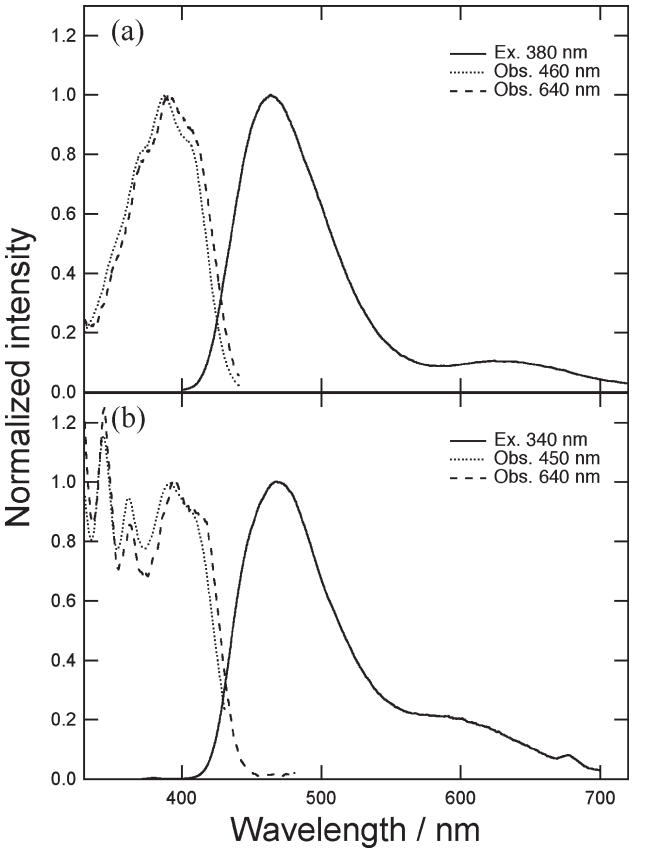

Figure 3. Fluorescence emission (—) and excitation spectra (··· and ---) of (a) 1PUA and (b) 2PUA in the presence of 10 mM TBAAc.

and dried in vacuo to yield 2-aminoanthracene (122 mg, 0.631 mmol, 4.7% yield) as a pale yellow solid. ^{1}H NMR (acetone-d_6, 270 MHz): δ 8.28 (s, 1H, anthryl), 8.05 (s, 1H, anthryl), 7.92−7.82 (m, 3H, anthryl), 7.38−7.25 (m, 2H, anthryl), 7.11 (d, 1H, J = 9.2 Hz, anthryl), 7.02 (s, 1H, anthryl), 5.05 (s, 2H, anthryl).

1-Anthracen-2-yl-3-phenylurea (2PUA). 2-Aminoanthracene (105 mg, 0.543 mmol) and phenylisocyanate (70 μL, 0.646 mmol) were stirred in dry THF (5 mL) at room temperature under N_2 for 22 h. The resulting precipitate was filtered off and washed with THF and dichloromethane to yield 2PUA (104 mg, 0.333 mmol, 61.1% yield) as a yellow solid. ^{1}H NMR (DMSO-d_6, 270 MHz): δ 8.96 (s, 1H, −NH), 8.79 (s, 1H, −NH), 8.48 (s, 1H, anthryl), 8.40 (s, 1H, anthryl), 8.27 (s, 1H, anthryl), 8.05−8.02 (m, 3H, anthryl), 7.52−7.40 (m, 5H, anthryl and phenyl), 7.31 (t, 2H, J = 7.7 Hz, phenyl), 7.00 (t, 1H, J = 7.4 Hz, phenyl); ^{13}C NMR (DMSO-d_6, 67.5 MHz): δ 152.4, 139.4, 136.5, 131.8, 131.6, 129.9, 128.8, 128.7, 128.0, 127.9, 127.4, 125.7, 125.4, 124.5, 124.2, 121.8, 120.8, 118.2, 111.6. Anal. Calcd for $C_{16}H_{21}N_2O$: C, 80.75; H, 5.16; N, 8.97; found: C, 80.93; H, 5.35; N, 8.96.

RESULTS

Absorption Spectra. Figure 1a shows the absorption spectra of 1PUA in DMSO with various concentrations of TBAAc (0, 1, and 10 mM). In the absence of TBAAc, the spectral shape was broad compared to that of the parent molecule, anthracene, with vibrational structure.[14] The maximum wavelength was 384 nm, with shoulders at 344, 363, and 405 nm. The characteristics of the absorption spectrum seemed to be similar to that of 1-aminoanthracene rather than unsubstituted anthracene.[14,19] The red-edge region (wavelengths longer than 380 nm) shifted to longer wavelengths (up to 440 nm) in the presence of 10 mM TBAAc, while the absorption band below 380 nm showed no shift, although there was a slight increase in absorbance.

As expected, the spectral shape of 2PUA was totally different from that of 1PUA, with strong vibrational bands from 320 to 380 nm, as shown in Figure 1b. In contrast to 1PUA, the red-edge absorption band (greater than 390 nm) was red-shifted in the presence of TBAAc, while the absorbance below 340 nm increased significantly. This indicates that the electronic state of 2PUA has a more complicated nature than that of 1PUA.

Fluorescence Spectra. Figure 2a shows changes in the fluorescence spectrum of 1PUA in the presence of TBAAc in DMSO. While the spectrum in the absence of TBAAc had a maximum at 460 nm, the fluorescence intensity decreased as the TBAAc concentration increased from 0 to 10 mM, followed by the appearance of a new band maximized at 620 nm, as shown in the inset of Figure 2a. The peak wavelength of 1PUA remained unchanged even in the presence of 10 mM TBAAc. The changes in 2PUA in the presence of TBAAc were different from those of 1PUA. An increase in the TBAAc concentration resulted in a decrease in fluorescence intensity and red shifting of the spectrum; in addition, a new emission band appeared, with a peak at 600 nm. The relative intensity of the new band compared to the LE emission of 2PUA was greater than for 1PUA. Since the peak wavelength of 2PUA was red-shifted as the concentration of

Table 1. Fluorescence Lifetimes of 1PUA in the Presence and Absence of TBAAc

	τ (ns)		
[TBAAc] (mM)	450 nm	650 nm	free[a] (%)
0	14.6 (1.00)		100
5	13.8 (0.38)	4.7 (1.00)	12.5
	0.3 (0.62)	0.1 (−1.00)	
10	10.6 (0.17)	4.4 (1.00)	6.7
	0.3 (0.83)	0.1 (−1.00)	

[a] Ratio of uncomplexed 1PUA to TBAAc. The values in parentheses are the normalized amplitudes for the respective lifetimes.

Table 2. Fluorescence Lifetimes of 2PUA in the Presence and Absence of TBAAc

	τ (ns)		
[TBAAc] (mM)	460 nm	640 nm	free[a] (%)
0	18.9 (1.00)		100
5	14.7 (0.08)	13.4 (1.00)	3.4
	5.0 (0.92)	4.0 (−1.00)	
10	13.1 (0.06)	13.4 (1.00)	1.7
	5.1 (0.94)	4.0 (−1.00)	

[a] Ratio of uncomplexed 2PUA to TBAAc. The values in parentheses are the normalized amplitudes for the respective lifetimes.

TBAAc increased, other emissive species were also expected to be present. Thus, it was concluded that there were three different emissive species for *n*PUA: one with no association between *n*PUA and TBAAc, the complex between *n*PUA and TBAAc, and a long-wave emission. Hereafter, the latter is referred to as ^{1}X*, by analogy with 9PUA.[13]

Excitation Spectra. Figure 3a shows the excitation spectrum of 1PUA in the presence of 10 mM TBAAc. The excitation spectrum observed at 640 nm was red-shifted relative to the spectrum observed at 460 nm, which indicates that the longer-wavelength emissive species (^{1}X*) has a electronic state different from that of the shorter-wavelength species. ^{1}X* may be the species in which 1PUA is associated with TBAAc, as it is consistent with the absorption changes in the presence of TBAAc, as shown in Figure 1a. This is also applicable to 2PUA, as shown in Figure 3b. Thus, the inclusion complex with TBAAc was concluded to be responsible for the different excitation behaviors.

^{1}H NMR Spectra. To confirm the complexation of 1PUA or 2PUA with TBAAc, ^{1}H NMR spectra were obtained in the absence and presence of TBAAc. This revealed the existence of hydrogen bonds between 1PUA and TBAAc, since downfield shifts of the NH protons from 9.13 and 8.97 ppm to 11.50 and 11.03 ppm were observed in the presence of TBAAc. These were attributed to the NH proton signals of one urea group and another urea group adjacent to the anthracene moiety, respectively (see Supporting Information, Figure S1). The equivalent signals in 2PUA also exhibited downfield shifts, from 8.95 and 8.79 ppm to 12.36 and 12.17 ppm, respectively. These shifts imply that *n*PUA interacts with TBAAc by hydrogen bonding through the urea moiety of *n*PUA.

Association Constants. The association constants of 1PUA and 2PUA with TBAAc were determined, according to eq 1, as 1.4×10^3 and 5.7×10^3 M^{-1}:[20]

$$\frac{I_0}{I - I_0} = \frac{I_0}{I_{max} - I_0}\left(\frac{1}{K_a[A]} + 1\right) \quad (1)$$

where I_0 and I are the fluorescence intensities of the host monitored at 450 nm in the absence and presence of anions, respectively, [A] is the total anion concentration, and I_{max} is the fluorescence intensity of *n*PUA fully hydrogen bonded with the anion. The difference in the association constants of 1PUA and 2PUA may arise from the acidity of the urea protons.[21,22]

Lifetimes of *n*PUA in the Excited State. The fluorescence decay of 1PUA in the absence of TBAAc under Ar gave a single-exponential curve with a lifetime of 14.6 ns (Table 1). The fluorescence curve observed at 450 nm in the presence of 5 mM TBAAc showed biexponential decay, with lifetimes of 13.8 and 0.3 ns, while the lifetimes at 650 nm showed rise and decay behaviors of 0.1 and 4.7 ns, respectively. In the presence of 10 mM TBAAc, the longer-lifetime component at 450 nm reached 10.6 ns, although the shorter-lifetime component remained constant at 0.3 ns. The decrease in lifetime from 14.6 to 10.6 ns may be ascribed to dynamic quenching by free TBAAc. Since the amplitude of the 0.3 ns component observed at 450 nm increased from 0.62 to 0.83 in the presence of 5 and 10 mM TBAAc, it may be attributed to a hydrogen-bonded complex of 1PUA with TBAAc. The lifetimes of 2PUA, observed at 460 nm, were 5.0 and 14.7 ns in the presence of 5 mM TBAAc, with quite a high amplitude (0.92) for the shorter-lifetime component due to the relatively high association constant, which is 4 times larger than that for 1PUA (Table 2). In contrast to this, the shorter lifetime was 16 times longer than the equivalent in 1PUA, reflecting the relatively slow quenching process of the 2PUA−TBAAc complex in the excited singlet state. This may reflect the intramolecular interaction between anthracene and the hydrogen-bonded urea moieties in the excited state. Since the observed rate constant was less than 30 ps for 9PUA, as estimated from the rising component of fluorescence at 580 nm, the rate constant seems to be related to the electronic interaction between the urea and anthracene moieties; the smaller the interaction, the lower the rate constant of proton transfer in the excited singlet state.

The time development of the new emission was confirmed by time-resolved spectra of *n*PUA (see Supporting Information, Figures S2 and S3). The buildup of new emission spectra, maximized around 650 and 640 nm, was confirmed at 0.1 and 4.0 ns for 1PUA and 2PUA, respectively.

DISCUSSION

Formation of Complex with TBAAc. As shown by the spectroscopic measurements, *n*PUA may form a complex with TBAAc through hydrogen-bonding interactions between the urea moiety of *n*PUA and the carboxylate group of TBAAc, which causes a red shift in the absorption spectrum, the appearance of a new emission band, and a downfield shift in the ^{1}H NMR spectrum. Comparison of the association constants indicates that 2PUA interacts with TBAAc 4 times as strongly as 1PUA.

The absorption spectra indicate that the electronic interaction between the anthracene and urea moieties of 1PUA is greater than that of 2PUA. DFT calculations for 1PUA showed a delocalized highest occupied molecular orbital (HOMO) compared to 2PUA (see Supporting Information, Figure S4). Since the HOMO orbital of 2PUA is similar to that of unsubstituted

Scheme 2. Resonant Structures of *n*PUA Depending on the Electronic Nature of the Substituent R[a]

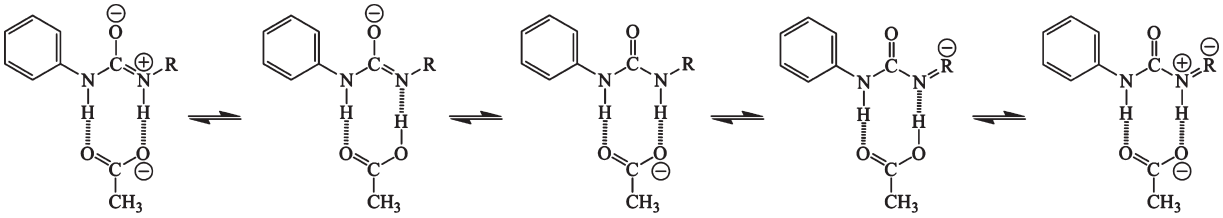

Electron-donating resonance Electron-accepting resonance

[a] R = 1- or 2-substituted anthracene.

anthracene, this is consistent with the vibrational structure of the absorption spectrum of 2PUA, which is ascribed to localized excitation in the anthracene moiety, in contrast to 1PUA. In general, the strength of hydrogen bonding depends on the acidity of the hydrogen donor.[21−23] The electron density of the nitrogen atom of the urea group adjacent to the anthracene moiety is lower in 2PUA than in 1PUA, since the anthracene moiety may work as an electron-donating group to the urea moiety. This indicates that the acidity may be higher in 2PUA than in 1PUA, which may be responsible for the larger association constant of 2PUA.[21,22]

Orbital Nature. The absorption spectra of 1PUA and 2PUA showed profiles similar to those of 1-aminoanthracene and 2-aminoanthracene, respectively. The localized n-orbital of the urea nitrogen can interact with the π-orbital of the anthracene moiety, leading to a πl, π^* orbital nature for the first excited singlet state, if the geometry of *n*PUA is planar.[24−26] Since the stable structure of 1PUA shows a small difference compared to that of 2PUA, based on DFT calculations, the electronic interaction between the urea and anthracene moieties may depend on the substituent position of the urea group relative to the anthracene group rather than on planarity between the urea and anthracene moieties.[27]

Origin of New Emissive Species (^{1}X*). The resonant structure of *n*PUA in the presence of acetate was inferred from a phenylurea compound, as shown in Scheme 2.[28] In general, the substituent R determines the charge density of each atom in the urea moiety. If R has electron-accepting ability, the resonance equilibrium may move to the right, as shown in Scheme 2; if R has electron-donating ability, it may move to the left. Since these resonances are allowed even in the ground state, as seen from steady-state spectroscopic measurement, a charge-transfer reaction may occur more efficiently in the excited singlet state than in the ground state.[29] Again, DFT calculations show that the urea moiety of 1PUA has an electron density that is consistent with a lack of LE absorption in the broad absorption spectrum, in contrast to 2PUA. This is supported by the observation that the molar extinction coefficient of 1PUA is twice as large as that of 2PUA.

For the purpose of discussing the emissive electronic state of *n*PUA, it is worthwhile to determine the spectral shapes of the ^{1}X*n** (n = 1, 2) emissions. An assumption was required to estimate these shapes from the fluorescence spectra; the spectral shape of the complex form was identical to that of free *n*PUA, except for the energy level of the corresponding emissive state. The emission shape of ^{1}X1* was derived by simply subtracting the emission spectrum of 1PUA in the absence of TBAAc from that of 1PUA in the presence of 10 mM TBAAc. Figure 2a shows that the complex of 1PUA with TBAAc may have almost no emissive properties, in comparison with the fluorescence behavior of 2PUA (Figure 2b), as there was no spectral shift and a monotonic decrease in emission with increasing TBAAc concentration. In contrast, determination of the spectral shape of ^{1}X2* required shifting the emission spectrum of 2PUA in the absence of TBAAc to the longer-wavelength side by 760 cm^{-1}; the spectral shape of the complex was derived by subtracting the spectrum of ^{1}X2* from that of 2PUA in the presence of 10 mM TBAAc. The resulting peak wavelengths of 1PUA and 2PUA were estimated as 640 and 600 nm (see Supporting Information, Figure S5). Although the method for determining the spectral shapes of ^{1}X*n** is based on an assumption, as mentioned above, the wavelengths of the emission maxima of *n*PUA may be used to compare the emissive states of *n*PUA. The emissive state of ^{1}X1* is stabilized by 1040 cm^{-1} relative to that of ^{1}X2*, which is consistent with the existence of more extended π-conjugation in 1PUA than in 2PUA.

The extended π-conjugation of anthracene with urea moieties may mean that anthracene functions as an electron-donating, rather than an electron-accepting, moiety. This may lead to the faster electron-transfer reaction in 1PUA compared with 2PUA. However, no explanation has yet been found for the difference between their time constants.

A plausible reaction scheme for 2PUA is shown in Figure 4. The electronic structure of ^{1}X*n** is still under consideration. As described above, the complex of 1PUA with TBAAc may be less fluorescent, with a lifetime of 100 ps, or have a spectrum similar to that of uncomplexed 1PUA. A major difference between 1PUA and 2PUA may arise from the variation in the substituted position of the anthracene ring. As seen from the DFT calculations, the electron density of the substituted 2-position of anthracene is less than that of the substituted 1-position, leading to weak interaction between the anthracene and urea groups. This may explain the slower formation of ^{1}X2* compared to ^{1}X1*, since the rate constant of the charge-transfer reaction depends on electronic coupling between the donor and acceptor moieties. Furthermore, in general, proton transfer takes place on an ultrafast time scale of less than 100 fs or even less than 1 ps. As far as we are aware, this is the first example of proton transfer with a rate constant as slow as 4 ns. One possible explanation for this slow reaction is delocalization of the excitation accompanying the formation of ^{1}X*n** triggered by proton transfer in the excited singlet state. If this were the case, it would demonstrate that the proton-transfer rate constant may be controlled by appropriate design of proton-transfer systems.

dx.doi.org/10.1021/jp2022693 |*J. Phys. Chem. A* 2011, 115, 8227–8233

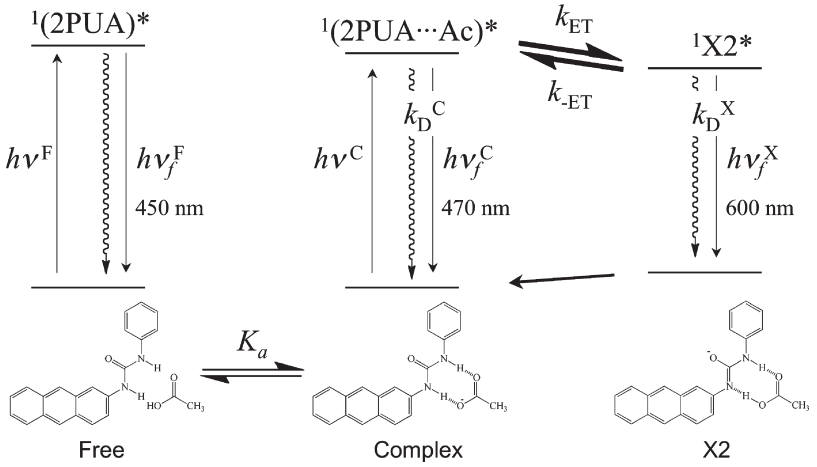

Figure 4. Reaction process of 2PUA in the presence of TBAAc.

Kinetic Analysis of the Formation and Relaxation of ^{1}X*n.** We may assume that there is reverse electron transfer from ^{1}X2* to the excited singlet state of the complex referred to as ^{1}(2PUA···Ac)*, with a rate constant k_{-ET} (as shown in Figure 4), since the longer-lifetime component observed at 460 nm is in good agreement with that observed at 640 nm in the case of 2PUA. If k_{-ET} has a significant value relative to k_{ET}, a two-state model may be used to analyze the kinetic rate constants involved in the excited state.[30,31] If we suppose $[^1(2PUA\cdots Ac)^*] = [^1(2PUA\cdots Ac)^*]_0 = 0$ at $t = 0$, the following equations allow us to perform calculations to determine the rate constants involved.[32−36]

$$\frac{[^1(2PUA\cdots Ac)^*]}{[^1(2PUA\cdots Ac)^*]_0} = \frac{1}{\gamma_1 - \gamma_2}\{(X - \gamma_2)\exp(-\gamma_1 t) - (X - \gamma_1)\exp(-\gamma_2 t)\} \quad (2)$$

$$\frac{[^1X2^*]}{[^1(2PUA\cdots Ac)^*]_0} = \frac{k_{ET}}{\gamma_1 - \gamma_2}\{\exp(-\gamma_2 t) - \exp(-\gamma_1 t)\} \quad (3)$$

where

$$\gamma_1 = \frac{1}{2}\{(X + Y) + \sqrt{(X - Y)^2 + 4k_{-ET}k_{ET}}\} \quad (4)$$

$$\gamma_2 = \frac{1}{2}\{(X + Y) - \sqrt{(X - Y)^2 + 4k_{-ET}k_{ET}}\} \quad (5)$$

$$X = k_D^C + k_{ET}, \qquad Y = k_D^X + k_{-ET} \quad (6)$$

$$\gamma_1 + \gamma_2 = X + Y = k_D^C + k_{ET} + k_D^X + k_{-ET} \quad (7)$$

The rate constants k_D^C and k_D^X are the deactivation constants, including radiative and nonradiative decay constants, for ^{1}(2PUA···Ac)* and ^{1}X2*, respectively. An iterative fitting method was applied to a deconvoluted decay curve to determine four unknown rate constants, which are correlated with eq 7, in the presence of 5 and 10 mM TBAAc, according to a previously reported calculation method using IGOR Pro 4.08J.[37] The resulting rate constants were independent of both the concentration of TBAAc and the monitor wavelength (Table 3; see also Supporting Information, Figures S6 and S7). This is why more than 96% of 2PUA can associate with TBAAc (Table 2). The formation rate constant of ^{1}X2*, k_{ET}, was determined to be about 4×10^7 s^{-1}, which was comparable to the reverse electron transfer rate, k_{-ET}, indicating nonnegligible regeneration of ^{1}(2PUA···Ac)* from ^{1}X2*. This is consistent with the appearance of fluorescence spectra emitted from the complex, as shown in the insets of Figure 2. Although the profiles of fluorescence decay for 1PUA monitored at 450 and 650 nm did not give lifetimes similar to those of 2PUA, the same procedure was applied to determine rate constants. In the presence of 5 mM TBAAc, no appropriate fitting was obtained for either the 450-nm or the 650-nm decay curve due to the considerable amount of free 1PUA (12.5%). The decay curve observed at 650 nm in the presence of 10 mM TBAAc also resulted in no fitted curve, which implied extreme difficulty in solving a time development profile comprising fast rise and slow decay. Accordingly, only the decay profile monitored at 450 nm was solved, giving values of 2.4×10^9, 4.7×10^8, 1.4×10^8, and 7.2×10^7 s^{-1} for k_{ET}, k_{-ET}, k_D^C, and k_D^X, respectively (see also Supporting Information, Figure S8). It is noteworthy that k_{-ET} was significantly smaller than k_{ET}. The difference between k_{ET} and k_{-ET} is allowed to explain the fact that 1PUA gives no detectable emission for a complex in the steady state fluorescence spectrum, as shown in the inset of Figure 2a. Consequently, the k_{ET} value of 1PUA is 2 orders of magnitude greater than that of 2PUA. A plausible explanation is that this reflects faster charge delocalization in 1PUA, arising from significant electronic coupling between the anthracene and urea moieties, which is consistent with the absorption spectrum and DFT calculations, as discussed in the previous section.

Table 3. Determined Rate Constants of 1PUA and 2PUA in the Presence of TBAAc

			rate constants (10^7 s^{-1})			
	[TBAAc] (mM)	λ_{obs} (nm)	k_{ET}	k_{-ET}	k_D^C	k_D^X
1PUA	10	450	240	47	14	7.2
2PUA	5	460	4.1	3.3	15	4.8
2PUA	5	640	5.5	4.5	17	4.6
2PUA	10	460	4.0	2.3	15	6.3
2PUA	10	640	5.7	5.3	18	4.0

However, the origin of the 2-order-of-magnitude difference in the k_{ET} values of 1PUA and 2PUA is still unknown.

In contrast, since k_D^C and k_D^X are independent of the substituted position of the anthracene moiety, it was concluded that the relaxation kinetics (except for electron transfer) are determined predominantly by the electronic properties inherent in anthracene in the excited singlet state.

CONCLUSIONS

The effect of substitution position on excited-state intermolecular proton transfer in the excited singlet state was investigated, and it was found that substitution position has a considerable effect on the proton-transfer rate constant. It was revealed that the charge density of the substituted position of the anthracene moiety determines the rate constant of the formation of new emissive species. However, the rate constant for the generation of new emissive species was found to be 2 orders of magnitude greater for 1PUA than for 2PUA, which was not expected based on the difference in charge density at the respective substituted positions.

ASSOCIATED CONTENT

Supporting Information. ^{1}H and ^{13}C NMR spectra, time-resolved spectra, DFT calculation results, and estimation of new emissive spectra. This material is available free of charge via the Internet at http://pubs.acs.org.

AUTHOR INFORMATION

Corresponding Author

*Tel.: +81-29-853-4315. Fax: +81-29-853-6503. E-mail: arai@chem.tsukuba.ac.jp.

ACKNOWLEDGMENT

This work was supported by a Grant-in-Aid for Scientific Research in a Priority Area "New Frontiers in Photochromism" (No. 471) from the Ministry of Education, Culture, Sports, Science, and Technology (MEXT), Japan.

REFERENCES

(1) Máñez, R. M.; Sancenón, F. *Chem. Rev.* **2003**, *103*, 4419–4476.
(2) Smith, P. J.; Reddington, M. V.; Wilcox, C. S. *Tetrahedron Lett.* **1992**, *33*, 6085–6088.
(3) Fan, E.; van Arman, S. A.; Kincaid, S.; Hamilton, A. D. *J. Am. Chem. Soc.* **1993**, *115*, 369–370.
(4) Nishizawa, S.; Bülmann, P.; Iwao, M.; Umezawa, Y. *Tetrahedron Lett.* **1995**, *36*, 6483–6486.
(5) Yamaguchi, S.; Akiyama, S.; Tamao, K. *J. Am. Chem. Soc.* **2001**, *123*, 11372–11375.
(6) Gunnlaugsson, T.; Davis, A. P.; O'Brien, J. E.; Glynn, M. *Org. Lett.* **2002**, *4*, 2449–2452.
(7) Ghosh, K.; Adhikari, S. *Tetrahedron Lett.* **2006**, *47*, 8165–8169.
(8) Boiocchi, M.; Boca, L. D.; Gómez, D. E.; Fabbrizzi, L.; Licchelli, M.; Monzani, E. *J. Am. Chem. Soc.* **2004**, *126*, 16507–16514.
(9) Kwon, J. Y.; Jang, Y. J.; Kim, S. K.; Lee, K. H.; Kim, J. S.; Yoon, J. *J. Org. Chem.* **2004**, *69*, 5155–5157.
(10) Jose, D. A.; Kumar, D. K.; Kar, P.; Verma, S.; Ghosh, A.; Ganguly, B.; Ghosh, H. N.; Das, A. *Tetrahedron* **2007**, *63*, 12007–12014.
(11) Jose, D. A.; Singh, A.; Das, A.; Ganguly, B. *Tetrahedron Lett.* **2007**, *48*, 3695–3698.
(12) Ghosh, K.; Sen, T. *Tetrahedron Lett.* **2008**, *49*, 7204–7208.
(13) Ohshiro, I.; Ikegami, M.; Shinohara, Y.; Nishimura, Y.; Arai, T. *Bull. Chem. Soc. Jpn.* **2007**, *80*, 747–751.
(14) Berlman, I. B. *Handbook of Fluorescence Spectra of Aromatic Molecules*; Academic Press: New York, 1971.
(15) Nishimura, Y.; Kamada, M.; Ikegami, M.; Nagahata, R.; Arai, T. *J. Photochem. Photobiol., A: Chem.* **2006**, *178*, 150–155.
(16) Boens, N.; Tamai, N.; Yamazaki, I.; Yamazaki, T. *Photochem. Photobiol.* **1990**, *52*, 911–917.
(17) David, G.; Wang, B.; Wasielewski, M. R. *J. Photochem. Photobiol., A: Chem.* **1996**, *102*, 71–80.
(18) Dahan, A.; Ashkenazi, T.; Kuznetsov, V.; Makievski, S.; Drug, E.; Fadeev, L.; Bramson, M.; Schokoroy, S.; Rozenshine-Kemelmakher, E.; Gozin, M. *J. Org. Chem.* **2007**, *72*, 2289–2296.
(19) Grabowski, Z. R.; Rotkiewicz, K. *Chem. Rev.* **2003**, *103*, 3899–4031.
(20) F.-Forgues, S.; Le Bris, M. T.; Guetté, J. P.; Valeur, B. *J. Phys. Chem.* **1988**, *92*, 6233–6237.
(21) Bowman-James, K. *Acc. Chem. Res.* **2005**, *38*, 671–678.
(22) Amendola, V.; Esteban-Gomez, D.; Fabbrizzi, L.; Licchelli, M. *Acc. Chem. Res.* **2006**, *39*, 343–353.
(23) Hay, B. P.; Firman, T. K.; Moyer, B. A. *J. Am. Chem. Soc.* **2005**, *127*, 1810–1919.
(24) Kasha, M.; Rawls, H. R. *Photochem. Photobiol.* **1968**, *7*, 561–569.
(25) Heldt, J.; Gormin, D.; Kasha, M. *Chem. Phys.* **1989**, *136*, 321–334.
(26) Nijegorodov, N.; Mabbs, R.; Winkoun, D. P. *Spectrochim. Acta, Part A* **2003**, *59*, 595–606.
(27) McRae, E. G.; Goodman, L. *J. Mol. Spectrosc.*. **1958**, *2*, 464–493.
(28) Bryantsev, V. S.; Firman, T. K.; Hay, B. P. *J. Phys. Chem. A* **2005**, *109*, 832–842.
(29) Tominaga, K.; Walker, G. C.; Jarzeba, W.; Barbara, P. F. *J. Phys. Chem.* **1991**, *95*, 10475–10485.
(30) Birks, J. B. *Photophysics of Aromatic Molecules*; Wiley-Interscience: London, 1970; p 301.
(31) Mataga, N.; Ottolenghi, M. *Molecular Association*; Academic Press: London, 1979; pp 1−78.
(32) Demas, J. N. *Excited State Lifetime Measurements*; Academic Press: New York, 1983; p 59.
(33) Okada, T.; Saito, T.; Mataga, N.; Sakata, Y.; Misumi, S. *Bull. Chem. Soc. Jpn.* **1977**, *50*, 331–336.
(34) Migita, M.; Okada, T.; Mataga, N.; Sakata, Y.; Misumi, S.; Nakashima, N.; Yoshihara, K. *Bull. Chem. Soc. Jpn.* **1981**, *54*, 3304–3311.
(35) Okada, T.; Migita, M.; Mataga, N.; Sakata, Y.; Misumi, S. *J. Am. Chem. Soc.* **1981**, *103*, 4715–4720.
(36) Hirata, Y.; Kanda, Y.; Mataga, N. *J. Phys. Chem.* **1983**, *87*, 1659–1662.
(37) Nishimura, Y.; Shimamura, K.; Ohmori, Y.; Shinohara, Y.; Arai, T. *J. Photochem. Photobiol. A: Chem.* **2011**, *218*, 69–75.